Lab on a Chip

TECHNICAL INNOVATION

View Article Online
View Journal | View Issue

Cite this: *Lab Chip*, 2016, **16**, 2198

Whole Teflon valves for handling droplets†

Olgierd Cybulski,*[a] Slawomir Jakiela[b] and Piotr Garstecki*[a]

Received 18th March 2016,
Accepted 4th May 2016

DOI: 10.1039/c6lc00375c

www.rsc.org/loc

We propose and test a new whole-Teflon gate valve for handling droplets. The valve allows droplet plugs to pass through without disturbing them. This is possible due to the geometric design, the choice of material and lack of any pulses of flow generated by closing or opening the valve. The duct through the valve resembles a simple segment of tubing, without constrictions, change in lumen or side pockets. There are no extra sealing materials with different wettability or chemical resistance. The only material exposed to liquids is FEP Teflon, which is resistant to aggressive chemicals and fully biocompatible. The valve can be integrated into microfluidic systems: we demonstrate a complex system for culturing bacteria in hundreds of microliter droplet chemostats. The valve effectively isolates modules of the system to increase precision of operations on droplets. We verified that the valve allowed millions of droplet plugs to safely pass through, without any cross-contamination with bacteria between the droplets. The valve can be used in automating complex microfluidic systems for experiments in biochemistry, biology and organic chemistry.

1 Introduction

Valves are indispensable parts of microfluidic systems. In droplet microfluidics,[1] valves are typically used to generate droplets of a required volume at the required instant, to direct and sort droplets between branching channels, to control splitting and merging of droplets and for execution of complex protocols on larger groups of droplets, as for example loading or retrieving droplets to and from a series of traps.[2] Due to the typically large footprint and significant cost of valves, designers of microfluidic systems try to minimize their number or place them outside the microfluidic chips so that each of the valves may work with only one type of liquid (either the continuous or the droplet phase).[3] This strategy works well for relatively simple systems. In larger systems, the operations on droplets may be performed simultaneously at many different locations in the microfluidic circuitry. All these operations, even if logically independent of each other, constitute a network of – literally – connected vessels: any operation performed in one block may affect the function of all the others. This is because all physical operations on droplets, in fact even their sole presence in a given channel, create additional pressure drops and variations in the rate of flow.

To avoid this mutual interference, the most fragile modules could be temporarily isolated by valves, enabling measurements or physical operations on droplets without any influence from the rest of the system. This necessitates introduction of valves into the microfluidic systems. Most importantly, it also imposes the requirement that the valves must allow the droplets to pass through without disturbing them.

As we outline below, these requirements pose a much more difficult challenge than in the case of controlling single phase flow. Designing a tight valve that does not interfere with the transported droplets is a difficult task, because droplets are typically prone to leave small residues, by pinning and wetting, in any complicated, sharp or uneven geometries they pass through. Furthermore, the valve should be equipped with sensors that can detect the presence of droplets to ensure that they will not be fragmented when the valve closes. In addition, the valve should react quickly, with short response times or at least with constant, repeatable delays. The switching of the valve should not generate pressure pulses nor rapid displacements of liquid. The valve should ideally preserve the intervals of the continuous liquid between droplets and should allow one to use as small intervals as possible.

Development of valves that could allow droplets to pass through, in microfluidic systems, has not gained much attention to date. Two major review articles on valves in microfluidics, the "Review of Microvalves" in 2006 (ref. 4) and the "Microvalves and Micropumps for BioMEMS" in 2011 (ref. 5), do not mention droplet systems at all, except for valveless platforms based on electrowetting or dielectrophoresis. The vast majority of the listed designs of valves are inappropriate for droplets. Channels that have varying lumens, chambers or other geometrical restrictions, as well as differences in

[a] *Institute of Physical Chemistry, Polish Academy of Sciences, Kasprzaka 44/52, 01-224 Warsaw, Poland. E-mail: olgierd.cybulski@gmail.com; Fax: +48 22 3433333; Tel: +48 22 3433405*
[b] *Department of Biophysics, Warsaw University of Life Sciences, Nowoursynowska 159, 02-776 Warsaw, Poland. E-mail: garst@ichf.edu.pl*

† Electronic supplementary information (ESI) available. See DOI: 10.1039/c6lc00375c

wettability between materials, may cause the passing droplets to break, to be trapped or to partially wet the walls, leaving residues that may cross-contaminate other droplets. Chambers and other open spaces, where droplets flow unconfined by walls, may cause delays and change the intervals between subsequent droplets in a stream or even change their sequence. Moreover, in most of the valves, it is hard to avoid the presence of droplets between moving parts during the process of closing – that could lead to disintegration and cross-contamination between droplets caught by moving elements of the valve. The closing and opening of a valve may also cause unwanted pulses of pressure, affecting the motion and positions of all droplets in the stream – this is a typical drawback of many diaphragm or membrane valves and all pinch valves.

Below, we review several types of valves that either have been or could be used for handling droplets.

1.1 Droplet-compatible valves in elastomers

Pinch valves[4,5] act by squeezing a section of flexible tubing[6] or by locally compressing the flexible material above a channel of a microfluidic chip made of PDMS.[7] Pinch valves are obvious candidates for handling droplets because, in their open state, the droplets flow through unmodified segments of the tubing or channel. In addition, these valves offer perfect tightness and zero dead volume. Still, the pinch valves require powerful actuators (as the force needed to close the valve is orders of magnitude higher than the product of pressure in the channel and its cross-sectional area), and above all, they bring on large displacement of liquid, pushed out from the pinched section of the tubing or channel. This causes flow that could interfere with precise operations on droplets in other parts of the system. In addition, the use of pinch valves is restricted to tubing and chips manufactured with elastic materials, capable of surviving many cycles of compression and relaxation without fatigue. On the other hand, such an elastic material can be easily used for designs that integrate the valves with microfluidic chips, made of the same material, and actuated by forces transmitted by pneumatic microchannels rather than mechanical plungers.

Pneumatic membrane valves, fully integrated into PDMS chips, were first introduced by Unger *et al.*[8] These multilayer valves are often referred to as "Quake valves", after Prof. Quake, the senior author of this project. Similar designs were then used for generation of droplets on demand.[9,10] The main advantage of this complicated technology is miniaturization and the potential of scalability, with examples including arrays of thousands of valves[11] or arrays of traps with valve-triggered release of droplets.[12] Pneumatically actuated valves were also implemented in single layer chips and used for selective sampling at an inlet,[13] forced merging[14] and splitting droplets into daughter drops of volumes controlled by the pressure applied to a pneumatic valve.[15]

All these designs benefit from excellent elasticity and other attractive features[16] of PDMS. They also share the shortcomings of this material, such as leakage of uncured oligomers,[17,18] absorption of small molecules (esp. hydrophobic) into the polymer bulk,[17,19] biofouling,[20] and swelling by most organic solvents.[18] Numerous surface modifications of PDMS were applied to improve its native properties.[21] New clear and castable elastomers have been proposed as a replacement of PDMS. Styrene–ethylene/butylene–styrene copolymers (SEBS)[22] and off-stoichiometry thiol-ene (OSTE)[23] may reach the hardness almost as low as PDMS while having much better resistance to solvents, whereas Ecoflex – the silicone elastomer family made by Smooth-On – is much more elastic and as such can be used for interfacing microfluidics with soft-robotics.[24–26]

1.2 Droplet-compatible valves in hard materials

Valves that rely on elasticity have also been implemented in hard plastics, including both thermoset resins and thermoplastic polymers, such as polymethylmethacrylate (PMMA), polycarbonate (PC), polystyrene (PS), cyclic olefin copolymer (COC) and many others.[27] However, the movable sealing element – usually a membrane – must be made of softer material. The integration of two different materials constitutes an additional challenge in bonding.[28–30] Often the bonding process requires modification of the surface of the polymer which introduces the additional risk of delamination of the modified layer and systematic degradation of the surface, especially on the repeatedly stretched elastic membrane.[29] Unfortunately, for the chemical compatibility and vulnerability to biofouling, the system is only as resistant as the weakest link, *i.e.* the worst or most sensitive material.

Hard materials, as well as their combinations with soft sealing elements, may also be used for implementing a separate class of valves, in which a short segment of the fluidic duct – a gate – is slid or rotated with respect to the adjacent segments of the microfluidic channel. The gate design is especially useful for multichannel valves and multiplexers (where one inlet is switched between many outlets). Hybrid rotary valves for application in microfluidics have been manufactured by microstereolithography with embedded rubber sealing[31] (the multiplexer) and by combining rotary disks of hard plastic (PEEK) with the softer PTFE[32] (multichannel switch valve). An interesting four-channel monolithic rotary valve, proposed by Luharuka,[33] comprises a bistable rotary mechanism: a disk and four thermoelectric actuators, fabricated as a planar component by deep reactive ion etching (DRIE) from silicon wafer. Lack of additional sealing elements causes small leakage: the valve allows for modulation of flow up to 100 : 1 (open : close). This precludes the use of such a valve for regulation of flow in a microfluidic channel of high hydraulic resistance (say, 1000 times larger than the resistance of the open valve itself) because the flow rate for the closed valve and for the open valve would be almost the same (1.1 : 1).

None of the abovementioned rotary valves were tested for the control of two phase flow. Judging from the design of the

gates and inlets, we expect that the limiting factor in the use of these valves for handling of droplets is the potential for unwanted pinning and wetting on the parts made of different materials. We also expect that the unsealed gap of the monolithic silicon valve and the associated flow may cause trapping and in consequence also pinning of fragments of the droplets passing through the valve.

1.3 Droplet compatible valves in fluorinated materials

Fluorinated polymers have recently attracted significant attention because they combine resistance to many organic solvents, biocompatibility, and very low surface energy, that translates into the "omni-phobic" wetting behavior. In view of the use of these materials in valves, these materials can be divided into two major groups: (i) fluoroelastomers,[34,35] usually not fully fluorinated, soft materials with limited resistance to solvents and harsh chemicals (yet still significantly better than non-fluorinated plastics and elastomers) and (ii) hard fluoropolymers, *i.e.* the most inert, non-sticking and chemically resistant materials ever synthesized.

Some of the fluoroelastomers, such as Sifel, Viton, and PFPE MDA,[27] share elasticity and processability of PDMS with some of the chemical properties of Teflon (including the resistance to hydrocarbons). Unfortunately, these materials are either opaque to visible light (as Sifel and Viton) or not as resistant to aggressive solvents[36,37] as Teflon. They may also swell upon exposure to fluorinated oils.[34,37]

Among commercially available "hard" fluoropolymers that could be useful in rapid manufacturing of microfluidic chips are both not fully fluorinated resins, such as Dyneon THV, and perfluoropolymers, such as perfluoroalkoxy polymer resin (Teflon PFA) and fluorinated ethylene propylene (Teflon FEP). Dyneon THV (grade 500) can be processed by hot embossing with a PDMS stamp and sealed by thermal bonding with another piece of Dyneon[38] at temperatures as low as 200 °C. Unfortunately, Dyneon is not resistant to many popular solvents, including ketones (the lower grades of THV may be completely dissolved in acetone). PFA and FEP present superior chemical resistance, similar to polytetrafluoroethylene (PTFE). They also have similar mechanical properties.[39] However, in contrast to PTFE, both FEP and PFA are transparent and may be thermally processed and sealed. They also have higher permeability to oxygen than other fluoroplastics:[40] 5.3 barrer for PFA at 25 °C and 4.6 barrer for FEP (for a comparison: 0.14 for PMMA, 1.4 for polycarbonate, and 600–780 for PDMS). FEP is slightly softer than PFA and PTFE;[39] thus, parts of a valve made from this material are easier to seal without additional elastic elements. FEP is also a popular material for production of small diameter tubing. With all these characteristics, both FEP and PFA are attractive materials for making valves.

Unfortunately, both of these materials are difficult to process outside specialized industrial plants. Thermal processing requires high temperature (over 300 °C) and the necessity of dealing with high thermal expansion (about 6% elongation from room temperature to melting temperature). Despite these difficulties, a technique for manufacturing whole Teflon chips has been established four years ago.[41] The features on the surface of PFA are created by hot embossing from a master made of modified PDMS (resisting temperatures up to 200 °C higher than the native PDMS). After embossing, parts of the chip are bonded in a hot press. This process deforms the cross-section of the microchannels. Depending on the aspect ratio, the deformation is moderate or severe.[41] The same or slightly modified protocol of bonding was also proven successful for bonding a chip made of nine layers of laser cut slabs of PFA[42] and for a chip consisting of three PFA layers, micro-patterned by hot embossing from a glass mold.[43] PFA can also be bonded with the aid of a thin layer of photocurable Teflon-compatible glue.[44]

Due to the limited resistance to repeated deformations, membrane valves made of Teflon[41,43,45,46] need larger membranes to achieve the same range of displacement as compared to PDMS valves. This makes it rather difficult to use membrane valves made of Teflon for handling the flow of droplets. In particular, valves proposed by Ren *et al.*,[41] with a membrane made of a 15 μm thick film of FEP, may not be suitable for droplets – we expect that long droplets would break when passing through an open valve due to the change in the lumen along the way. Droplets could also get trapped in the dead volume of the valve.

Another challenge in designing a valve suitable for handling droplets is its connection with other parts of the system without any gaps, dead volumes or step-wise changes in the cross-section of the channels. Neither the connections should present any additional sealing material that could enhance pinning or wetting by the droplet liquid. The need for developing droplet compatible valves and droplet compatible fluidic connectors both fall into the same modular concept of the design of the systems.[47] It is thus a good idea to design the valve and connector in one, as an element of a systemic platform for processing droplets.

2 Results and discussion

Here, we report the first whole Teflon valve for handling droplets, free of all of the above-mentioned drawbacks. The valve is suitable both for the use in biotechnological applications of droplet microfluidics, that typically use water in oil emulsions, and in synthetic chemistry, as it is resistant to most of the aggressive organic solvents. The valve is easy to integrate with a modular droplet microfluidic platform (proposed in sec. 2.6) and can also be integrated into multilayer whole-Teflon microfluidic devices.

2.1 Selection of the architecture of the valve

We have considered and tested three different concepts of a valve, as illustrated in Fig. 1. In all of these designs, the valve in the open position forms a fluidic duct of a constant cross-section along its length. In addition, in all the concepts, closing the valve does not displace any liquid into the channel.

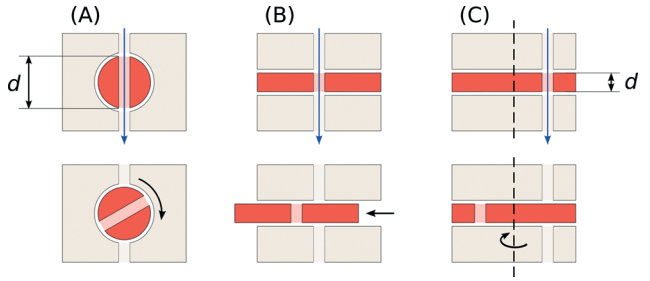

Fig. 1 Three architectures of valves for guiding droplets. The schematic illustrations show the valves in their open (top row) and closed (bottom row) states: (A) rotary plug valve, (B) sliding gate valve, and (C) rotary disk valve. Exaggerated clearances show the possible passages for leaks.

The first design, a rotary plug valve (Fig. 1A), comprises a cylindrical rod that can be rotated around its axis. The rod has a through channel drilled perpendicularly to the axis of rotation. Aligning the through-hole in the rod with a channel in the socket opens the valve, just as in a traditional stopcock valve. Tightness of this valve must be provided on the curved (cylindrical) surfaces of the rotary plug and its socket. In the subsequent designs, the movable segment with a through-hole is slid by purely translational motion (Fig. 1B) or rotated around an axis that is parallel to the fluidic channel yet not aligned with it (Fig. 1C). The tightness must be ensured on the contact between flat (planar) surfaces. For a large distance between the gate and the axis of rotation (*i.e.* much larger than the diameter of the gate), the difference between designs B and C is not significant – however, it affects mechanical details of the implementation. As it was mentioned in the introduction, the ideal valve for droplet microfluidics should allow for short intervals between droplets. It corresponds to the minimization of the length d (see Fig. 1), unless one opts to close the valve with droplets inside the gate.

After manufacturing and testing several prototype valves based on all three ideas (A, B and C), we decided to choose design C for the following reasons: (i) in B and C, the key surfaces providing both internal and external tightness may be native surfaces of commercially available prefabricates: sheets or plates with a smooth surface finish, while in A at least one surface must be machined – provided that we can buy a smooth, perfectly axisymmetric rod. (ii) In A, any deviation in the diameter of the cylindrical rod or its socket results either in losing tightness or increasing friction between the sealed surfaces, whereas in B and C, the exact dimensions of the parts are much less critical, as the surfaces may be pressed together with an external, normal, force. (iii) In B and C, the shortest potential leakage path of the closed valve increases with the distance traveled by the sliding or rotating gate and may be much larger than its thickness, d, whereas in A it cannot exceed $\pi d/2$. It means that for a fixed d, valves B and C would be much tighter (less leaky) than A, even if all the working surfaces were manufactured with the same precision and roughness (in fact, they are not – see point (i)). (iv) In A, d must be larger than the diameter of the fluidic channel, whereas in B and C there are no geometric reasons to limit d from below. However, another limitation of the minimum thickness of the sliding element or rotary disk (as well as of the minimum diameter of the rotary plug) is imposed by the required strength of these mechanical components against stresses induced by friction. (v) Although designs B and C share the same advantages over A, the practical implementation of C is less demanding and easier to seal from the external world – for this reason, we decided to continue with the design shown in Fig. 1C.

2.2 Design and assembly of the valve

Fig. 2 shows the schematic of the valve. The core elements of the valve (the rotary disk between two covers, see Fig. 1C) are made of FEP Teflon. These parts are embedded in a chassis composed of a number of supporting parts that provide mechanical stability and isolate the fluidic path through the valve from the external environment. The whole valve comprises a stack of five layers: the central layer (shown in Fig. 2A, in the middle of the cross-sectional view in Fig. 2B, and at the top of Fig. 2C), internal covers (two identical copies) and external covers (two almost identical). All the layers are pressed together with mounting screws and sealed with rubber O-rings. Importantly, the O-rings also serve to balance the mechanical stresses – see sec. 2.4. Fig. 2C shows an exploded view of the bottom three layers of the valve together with all the O-rings and the FEP tubing.

The central layer consists of a rotary disk placed in the middle of a fixed spacer of the same thickness (as shown in the upper right corner of Fig. 2C). Both the disk and the spacer are cut in a single process from the same sheet of FEP (see sec. 4), to minimize the effects of potential variation in thickness between different plates. The horizontal planes of the disk and of internal covers are not machined to preserve the smoothness of the prefabricated slabs. The angle of rotation of the disk is limited by the complementary indentations in the disk and the spacer – one of the extreme angular positions of the disk corresponds to the fully open state. The torque needed to rotate the disk is transmitted by a steel shaft with an additional pin extending perpendicularly to the shaft and inserted into a matching slot on the top surface of the disk.

The internal covers are cut from an FEP sheet of the same thickness as the central layer, whereas the external covers should be made of a thicker and stiffer material such as aluminium, polycarbonate or PMMA. For the application in droplet microfluidics, at least one of the external covers should be equipped with a fiber optics sensor, and for this reason, opaque materials are preferred. At the same time, transparent covers allow visual inspection of the inner layers, most importantly, of the position of the through-hole in the rotary disc. For this reason, we use two different external covers: one made of transparent plastic and the second, with an integrated optic fiber sensor, from black PMMA. In addition, we made the opaque (black) cover plate larger than that

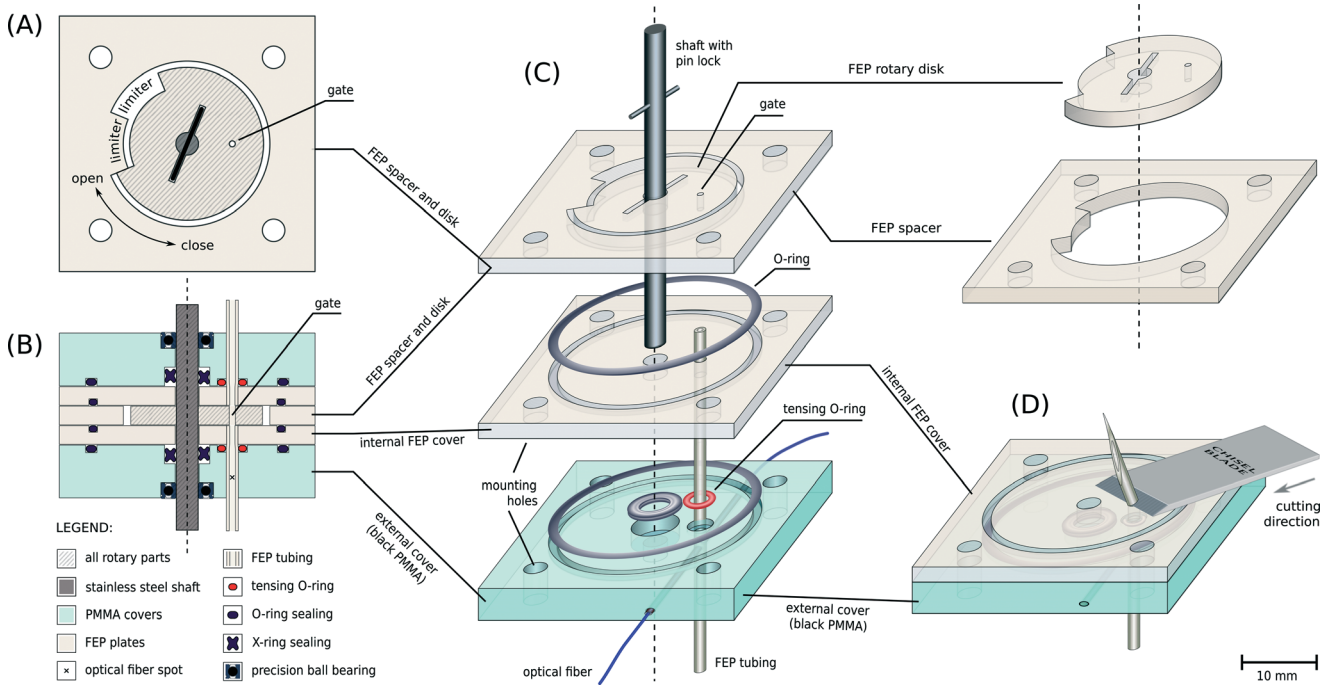

Fig. 2 Schematic drawings of the valve: (A) top view of the central layer comprising the rotary disk with a through-hole (gate) and a complementary immobile spacer, both made of FEP; (B) cross-section of the valve (all layers): the central layer with the rotary disk is placed between two internal covers (made of FEP) and two external covers made of a stiff polymer or metal; (C) 3D drawing of 3 of 5 layers from the central layer to the most bottom layer (the missing two layers are simply copies of the shown covers, flipped upside down); (D) method of pulling the FEP tubing through the covers and cutting it in the plane of the top surface of the internal cover.

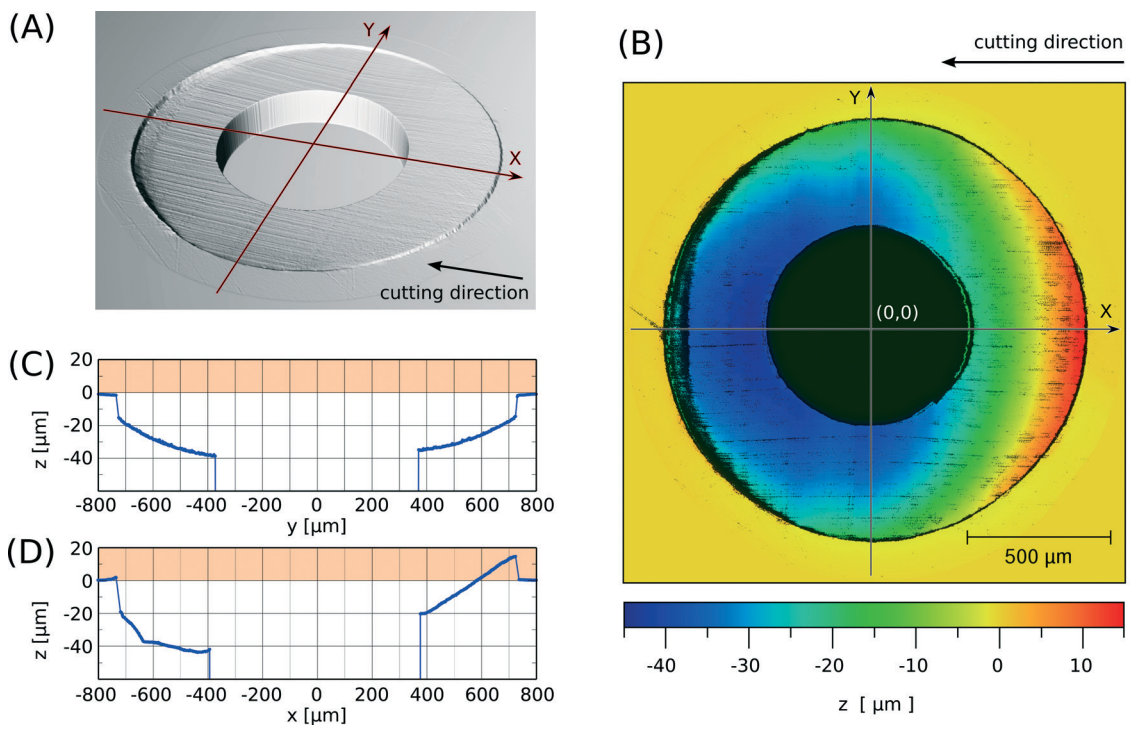

Fig. 3 The micro-topography of the surface of the internal cover after cutting the tubing in plane with this surface: (A) 3D visualisation of the profilometric data; *Z* axis in scale with *X* and *Y*. (B) Profilometric map of the cut, with $z = 0$ at the surface of the cover; black spots in the map have not been sampled due to noises or out-of-range errors. Profiles (C) across ($z(y)$) and (D) along ($z(x)$) of the cut. Note the protruding jaw at the line of the first contact with the knife, resulting from deformation of the tubing under the cutting edge.

shown in Fig. 2 to provide ample space on the side of the valve for mounting a small RC servomechanism to rotate the shaft and actuate the valve. See sec. 4 and the ESI† for additional information regarding the driving mechanism and a photograph of the valve in Fig. 4B.

The fluidic channel through the valve comprises the central through-hole in the rotary disc and two closely adjacent pieces of FEP tubing passing through tight holes in the covers. The tips of these two sections of the tubing match the position of the through-hole in the open state and become parts of the sealing surfaces adjacent to the rotary disk in the closed position.

2.3 Placing and cutting the tubing

In order to ensure external tightness and mechanical stability against accidental pulling out of the sections of the tubing from the valve, the diameters of the holes in the covers are substantially smaller than the outer diameter of the tubing. The nominal OD of the tubing is 1.60 mm, whereas the diameters of the holes in the outer and inner covers are 1.58 and 1.48 mm, respectively. Due to the significantly undersized hole in the inner cover, the terminus of the tubing remains aligned with the surface of the inner cover even if both the covers are moved apart from each other during assembly and disassembly of the valve.

Placing the tubing in the covers requires a special procedure. We first cut the end of the tubing at a very sharp angle (almost in parallel to the axis of the tubing). We then push the resulting long sharpened tip of the tubing through the holes in the external and internal covers, placing the 'tensing' O-ring between the covers. Then, we catch the tip of the tubing with pliers and pull at least several centimeters of the tubing through the holes. Then, the excess segment of the tubing above the internal cover is cut in such a way that the resulting cutting plane is as flat and as coplanar with the surface of the cover as possible. Importantly, the smooth surface of the cover cannot be scratched during cutting. After many tests with different methods, we recommend to cut the excess tubing with a razor sharp single bevel chisel blade (see sec. 4 for details). Straight and long razor blades and replaceable blades for paper knives may be used as well; however, due to the double-side polishing, they must be used with a proper tilt angle. This requires significant dexterity yet may provide equally good results. The procedure for placing and cutting the tubing on the covers is illustrated in Fig. 2D. Any scratches on the surface may compromise the tightness. Positive deviations (bulges) may increase the distance between covers and systematically scratch the surface of the rotating disc. Both bulges and indentations, as well as whiskers or burrs at the edge of the internal wall of the tubing, may cause disintegration of droplets and transfer of material between consecutive droplets passing through the valve.

2.3.1 Measuring the deviations of the cut surface. Fig. 3 shows a typical result of the process of cutting the tubing in plane with the surface of the cover. A properly executed cut

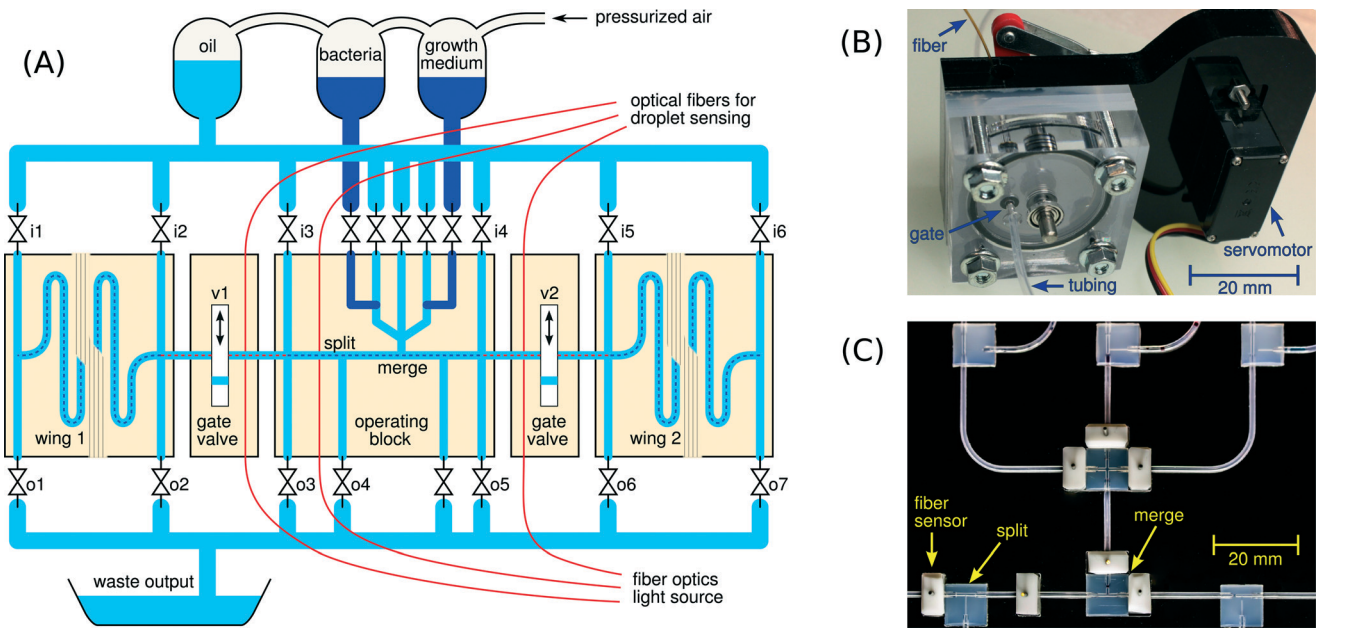

Fig. 4 Micro-droplet chemostat system used for testing the valves. (A) Simplified schematics. The droplets shuttle back and forth along the main channel, marked with a dashed line, or within its separate stages: the side incubation segments (wings, not drawn to scale as they are in fact 100× longer) and the operating block in the center. The directions of flows and other operations are controlled by inlet valves i1–i6, outlet valves o1–o7, and gate valves v1 and v2 (being the main subject of this article). The operating block allows for splitting of the droplets in required proportion or merging them with other droplets prepared on the spot from the growth medium and other (not shown) factors. Gate valves v1 and v2 isolate the operating block and protect it from the impact of the flow of liquids in the side wings (incubation sections). (B) One of the two gate valves. (C) Part of the operating block with modular FEP T-junctions used for splitting and merging droplets. White Teflon modules serve as holders for fiber optic sensors.

does not scratch this surface; thus, the only significant deviations from the plane are in the cross-section of the tubing itself. These deviations involve sub-micrometer furrows along the direction of the cut and, much more importantly, a systematic inclination of the surface along the cut: the beginning of the cut is elevated to +15 μm above the surface of the cover, while the middle section and the end of the cut are depressed down to −40 μm with respect to the plane of the cover. The extent of this systematic variation depends on the type and sharpness of the knife and on external forces applied to the protruding segment of the tubing during the cut. To minimize this variation, the free end of the tubing should be supported from the side opposite to the cutting direction, so that it cannot lean on the cover at the final stage of cutting. After experiments with several valves, we found that the bulges of the order of +15 μm do not scratch the surface of the disc. We hypothesize that these bulges are squeezed back into the hole in the cover when the valve is fastened with the mounting screws.

2.4 Tightness

In order to check both the internal and the external tightness of the valve, *i.e.* to verify that there are no leakages between the ports of the closed valve and from the inside to the outside of the valve, we immersed it in water and connected one of its inlets to compressed air at a pressure of 1 bar, whereas the second inlet was either (i) left free under the surface of water for closed valve or (ii) blinded, when the valve was open. We observed no bubbles within the time of over 15 minutes for each test, performed first on a freshly assembled, dry valve and then repeated after the valve was used with fluorinated oil. Although the presence of a thin film of this oil may lubricate the covers and prevent them from abrasion, we do not recommend tightening the mounting screws of the valve too much, as it may increase friction between the rotating disk and the covers and shorten the lifetime of the driving servomechanism. In our tests, the torque needed to rotate the main shaft of the valve was below 0.1 N m.

2.4.1 The role of rubber O-rings. As shown in Fig. 2, the valve contains eight different sealing elements made of synthetic rubber: there are four large O-rings between each pair of adjacent layers (of a diameter significantly larger than the diameter of the rotary disk), two X-rings (also known as quad-rings) between the steel shaft and cylindrical sockets in the external covers, and two small O-rings placed around the tubing between internal and external covers, beneath the movable disk. Normally, none of these sealing elements are in contact with the transmitted liquids and only the smallest O-rings (shown in red in Fig. 2) are indispensable for sealing the valve – they act as springs, pressing the internal covers against the movable disk *only* in the small neighborhood of the tips of the tubes. The region of the elevated clamping around this O-ring is large enough to seal the valve, yet small enough to not cause excessive friction between the clamped surfaces. In addition, the remaining O-rings (around the circumference of the rotating disk) play role of springs: they help to control and distribute the mechanical stresses in the FEP modules of the valve and create friction between layers, protecting them from unwanted sliding. The X-rings around the shaft of the valve protect the interior of the valve from external contaminations. In the absence of any X-rings or O-rings besides the smallest ones, the valve could still be sealed, yet the clamping force provided by mounting screws would be either too small to stabilize the assembly against skewing forces (parallel to the layers) or too high to enable rotation of the disk.

2.5 Droplet sensing

One of the outer covers, made of black PMMA, comprises a couple of optic fibers, placed in a channel drilled perpendicularly to the axis of the tubing. We first glued the fibers into segments of steel hypodermic needles and then cut and polished the tip of the fiber together with the tip of the needle. The needles facilitate insertion of the fibers into the guiding channels and press them tightly against the wall of the tubing, so that the sensor is mechanically stable against bending of the fibers and effectively isolated from external light. The optic fiber may serve two functions. The most important one for the use of the valve in droplet microfluidic experiments is to detect droplets. This is to assure that there are no droplets inside the working parts of the valve when it is changing its state. In addition, the fiber may be used to measure the optical density of the liquid inside the droplets. With a proper choice of the light source and of the sensor, fluorescence from the droplets may also be measured.

A range of different optoelectronic detectors may be used, depending on the required sensitivity, dynamic range and robustness to noise. For sensing the presence of droplets, we recommend – for the simplicity of the design and for high gain – the three-pin light to voltage converters of the family TSL257 and TSL257T (ams AG, formerly TAOS). These sensors combine a photodiode and a transimpedance amplifier into a simple, low noise, chip. Any white or color LED may be used as the light source. We recommend to tune the output signal of the sensor to the middle of the scale (2.5 V) for the pure continuous liquid. Due to the difference in the refractive indices between oil and droplets, the AD converter may then effectively measure the deviations from this level caused by the presence of the front, middle or end of the droplet within the detection window. One must also take into account the delays between the detecting signal and physical closing of the valve; however, the details of the control system and mechanical drive of the valve are out of the scope of this article.

2.6 Practical tests: the micro-droplet chemostat system

Below, we describe two tests of the performance of our valve in biotechnological applications. Two valves of this type are used as a part of the micro-droplet chemostat system, as shown in Fig. 4. This experimental platform serves as a basis for culturing and monitoring the evolution of a large number

of independent populations of living microorganisms encapsulated in microliter droplets. The first generation of this system[48] was made in a single polycarbonate microfluidic chip and used hexadecane as the continuous liquid. Although successful under anaerobic conditions, it could not be used for long lasting experiments with aerobic bacteria. Moreover, the necessity of using a surfactant (Span-80) highly exceeding the critical micellar concentration (which is below 0.06% w/w[49]) introduced the risk of cross-contamination, especially at longer times of culturing. To overcome these limitations, the micro-droplet chemostat system described here is made entirely of FEP Teflon and uses fluorinated oil for the continuous phase. Fluorinated oils are known for their excellent biocompatibility and solubility of oxygen.

The system has a modular architecture built with FEP tubing (ID = 0.8 mm) and simple custom made connecting modules: T-junctions and X-junctions drilled in FEP sheets of the same type as those used for the internal layers of the valve. The connectors have through holes of the same ID as the tubing and wider fittings for the tubing, leaving no gaps nor step changes in the cross-section of the fluidic duct between the tubing and the connector. We monitor the droplets with custom made fiber sensors. The sensor modules have through-holes that allow the tubing to be pulled through and perpendicular channels for the optic fibers. These sensor modules can be freely slid along the tubing to a desired position as shown in Fig. 4C. Due to the modular architecture, introducing small modifications as well as adding new functionalities to the system is much easier than in a typical, highly integrated microfluidic system.

We supply the system with the continuous phase (oil) and all other liquids (see sec. 4.2 for details) from pressurized containers shown schematically at the top of Fig. 4A. The waste (output) is kept under atmospheric pressure. All flows are controlled with three groups of valves: (i) the inlet valves (i1 to i6 and unmarked valves in between), (ii) outlet valves (o1–o7), and (iii) internal gate valves (v1 and v2 – as described above). The inlet valves work exclusively with oil or one of the droplet liquids and are connected to the microfluidic system *via* long, narrow capillaries, whose hydraulic resistance is much larger than a typical resistance of the driven system. This architecture ensures that the rate of flow through an open valve depends to a very good approximation only on the pressure in the container and not on the content and flow in the microfluidic system.[50,51] The outlet valves do not need any resistive capillaries. The system can be best controlled when the resistance of the valved outlets is as small as possible, to minimize the fluctuations of flow rate and pressure in the system caused by the leaving droplets.

The whole system is designed to generate a series of droplets, each containing a given combination of suspension of bacteria, media and solutions of active compounds (*e.g.* antibiotics). Then, the droplets are cycled back and forth in the long side channels and monitored for the optical density of the colony in the droplet. After a given time, or as directed by the pre-programmed control system, each of the droplet can be split, with a part of it going to waste and the second part being merged with a droplet containing fresh media and possibly a new concentration of an active substance. These two processes are quite distinct. Incubation happens over extended periods of time and both conceptually and technically is a simple process – requiring only a periodic change in the direction of flow. In contrast, the exchange of media is performed rarely and rapidly, yet requires significant precision in the control of flow of all the liquids. During these operations, it is highly preferred to isolate the central part from the two parts devoted for incubation. This isolation is achieved by using the droplet-compatible gate valves (Fig. 4A).

During the incubation, droplets are kept in constant motion, so that they are always surrounded by a film of continuous liquid. This is to provide systematic mixing and – first of all – to reduce the risk of cross-contamination, resulting from even minimal wetting of walls of the tubing by the droplet liquid or from adhering bacteria to these walls.[52] The direction of flow is controlled by side channels and corresponding inlet/outlet valves. For example, opening valves i1 and o2 in the left wing causes the droplets in this block to flow to the right, whereas opening i2 and o1 enforces the opposite flow direction. Due to the fiber optic sensors (only 3 of the total 25 are shown in Fig. 4A), the control automatically "knows" when to switch the flow directions to prevent droplets from escaping into the outlets.

The operating block in the center of the device is about 100× shorter than the wings (the wings are not drawn to scale, as shown in Fig. 4) and enables the following operations: (i) optical measurements on droplets in the flow, or during a short halt, (ii) generation of fresh droplets containing medium, bacteria, and growth factors, (iii) introducing these droplets into the main stream, (iv) merging them with the existing droplets in the main stream, (v) splitting the existing droplet into two parts and (vi) directing one of these parts or the whole existing droplet to the waste outlet.

After the population in a given droplet has multiplied to a set threshold density, as indicated by the optical density, the system begins the exchange of media in that droplet. A fraction of volume of this droplet is directed to waste, while the remaining part is replenished with fresh nutrients and other factors. The protocol of exchange comprises five operations: the measurement of optical density (to decide whether the droplet is ready for exchange), splitting of the droplet, generation of a droplet with fresh nutrients, merging it with one of the daughter droplets, and directing the second one to waste. The system allows culturing of over 200 independent colonies of bacteria for weeks of continuous operation, spanning several tens of thousands of generations of the microorganisms. This capability may find use in the research on mechanisms of emergence of drug resistance and on directed evolution of bacteria. The successful long-term operation of this system hinges on two conditions. First, the operations (splitting, generation, merging) on the droplets must be precise. Large

errors would quickly build up and hinder control over the composition of media and state of the culture. Second, there cannot be any cross-contamination between the droplets, as it could mix the colonies and spoil the idea of running a large number of independent experiments in parallel. Below we present two tests which demonstrate the role and quality of our gate valves in successful implementation of this experiment.

2.6.1 Isolating and splitting the droplets in the operating block. The operations of splitting and merging of droplets are performed in the central part of the system, at the T-junctions shown in Fig. 4C. Manipulation of the droplets is controlled remotely – through the external valves i3–i4, o3–o5 and unnumbered valves placed between them in Fig. 4A. Control of positions and volumes of processed droplets is provided by fiber optic sensors. The sensor shown in the lower left corner of Fig. 4C is used to assist splitting of the droplets. The same sensor, marked as fs2, is also shown in Fig. 5, which illustrates the sequence of operations required to controllably split a droplet. The procedure of splitting starts when the droplet passes valve v1 and is detected by sensor fs1 (embedded in the valve). Here, we assume that gate valve v2 is closed and the liquid flows to outlet valve o4. Within a specified interval after fs1 senses the passage of a droplet, the control automatically closes valve v1. This stops the droplet at a position marked in Fig. 5A. This position is not exactly known – it depends on a number of uncontrolled factors, including the positions and viscosities of all droplets occupying the left incubation wing. However, as the operating block is now isolated by gate valves v1 and v2, the precision of further operations is increased. After opening valve i3, the droplet continues with precisely controlled speed, and when it reaches sensor fs2, the subsequent steps of the splitting protocol are based on preprogrammed intervals, as shown in Fig. 5B–D.

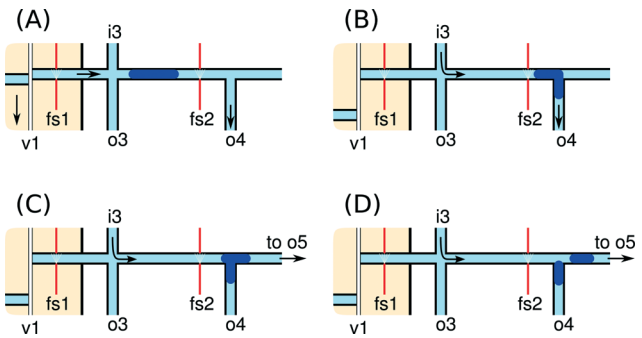

Fig. 5 Subsequent stages of splitting the droplet in the operating block. (A) Gate valve v1 starts to close within a specified time after passing fiber sensor fs1. (B) Precisely controlled oil flow from valve i3 to o4 (other valves of the operating block are closed) pushes the droplet partially into the side channel, by a fraction defined by a time interval elapsed after reaching sensor fs2. (C) After closing o4 and opening o5, a part of the droplet remaining in the main channel moves further to the right and finally (D) breaks away, leaving the detached part in the side channel (to be directed to waste).

We quantified the gain in precision introduced by the use of the droplet valves directly by measuring the variance of volume of the split droplets with and without the use of the droplet valves (Fig. 6). The performance of splitting without the valves was tested for two different numbers of circulating droplets: a small set of 10 droplets and a large set of 200 droplets. The test with valves was made for 200 droplets. We plot the standard deviations for 50 independent trials for each split volume, normalized to the original volume (6.4 μL). The isolation of the operating block significantly improves the precision of splitting, especially in the case of long trains of droplets in the tubing. The dependence on the number of droplets was observed only for the case without gate valves, and it results most probably from additional hydrodynamic resistance introduced by droplets flowing in the wings of the system.

2.6.2 Cross-contamination. To verify the ability of the system to cycle droplets without cross-contamination (still in the same system from Fig. 4) over extended periods of time, we generated 200 droplets of identical size and separation along the tubing and seeded 180 of them with bacteria. The remaining 20 droplets (10 on each end of the series) served as a control group. These droplets were cycling back and forth in the same way as the seeded droplets, and in particular, they all flowed two times per cycle (*i.e.* once per minute) through both of the droplet valves. We monitored the density of bacteria (*via* the measurement of optical density) in each droplet in each cycle. In addition, each droplet was periodically replenished (either in half-hour intervals or if the optical density reached the level of 0.5). A droplet selected for replenishment was isolated in the operating block with the droplet valves, half of the droplet was removed to waste and the remaining half was merged with the same amount of fresh medium. Within the first hours of the experiment, all seeded droplets reached the required optical density of 0.5. During 80 hours of the experiment, each of the 200 droplets was replenished at least 160 times. The seeded droplets were

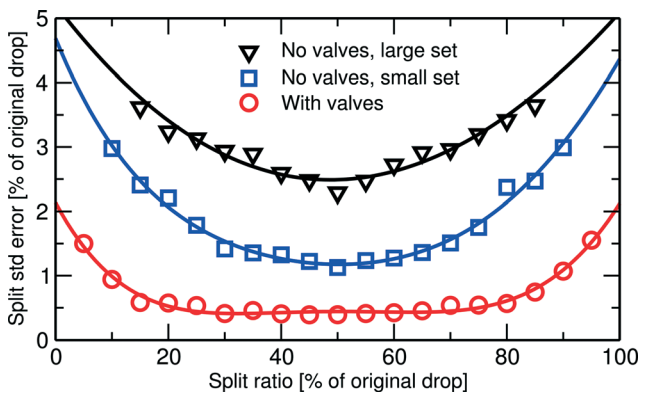

Fig. 6 Volume errors in splitting *versus* intended splitting ratio; without the use of gate valves for a large (200) and a small (10) set of droplets handled at the same time, and with the use of gate valves (for 200 droplets; however, due to the valves, the number of droplets is irrelevant).

replenished more often, because the time of growth of the colony from an optical density of 0.25 (resulting from the substitution) to 0.5 was about 20 minutes. Anyway, in the course of the experiment, each of the droplet valves was actively used (*i.e.* closed in between passing droplets and open again) more than 40 000 times with more than one million passages of droplets through the open valves. Within this time, we observed no sign of any cross-contamination of the originally empty droplets.

After 80 hours, one of the droplets that contained a colony of bacteria was improperly interpreted by the fiber optic sensor, and in consequence, this droplet was chopped by the gate valve. This moment is selected as $t = 0$ in Fig. 7, presenting the evolution of the optical density in one of the control droplets (not seeded at the beginning of experiment). As shown, jamming of the droplet with bacteria promptly contaminated the control droplet and started a colony that grew in the same manner as the colonies in the droplets seeded at the beginning of the experiment. All the remaining 19 control droplets were also contaminated with bacteria within 50 minutes of the incident. This experiment shows that – if not for an error in the control system – the valves allow for a contamination-free operation of the system over very long intervals and millions of passages of droplets, in spite of the very high sensitivity of the system to contamination.

It is not clear what is the exact mechanism of the cross-contamination. For sure, the droplet was chopped by closing the gate, and this produced many smaller droplets, including microdroplets, which could get stuck in small nooks of the micromachined surfaces. It is also plausible that some of the bacteria from the destroyed droplet clung to the rough surfaces of the machined walls, creating hydrophilic spots that could be wetted and picked up by other droplets. Interestingly, after the incident, the valve continued to contaminate droplets with bacteria. Even in subsequent experiments, all droplets of clean medium became contaminated after the first pass through the contaminated valve. Autoclaving the valve solved the problem.

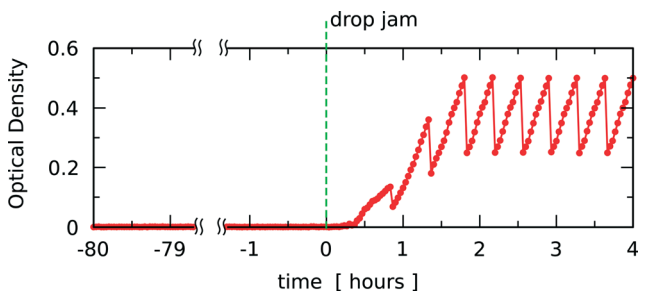

Fig. 7 Evidence of cross-contamination resulted from jamming a single droplet in the gate of the valve during closing, after 80 hours of normal work with 200 droplets, of which 180 were populated by bacteria and 20 control droplets remained clean. After jamming one of the droplets with bacteria at time 0, the microorganisms populate all control droplets, reaching the stationary concentration after about 2 hours. The optical density of one of the control droplets as a function of time is shown.

3 Concluding remarks

We presented a simple and functional design of an automated, whole Teflon valve for controlling the flow of droplets. Plugs of non-wetting liquid may flow through the open valve without being disturbed in any way, just as they would be flowing through a segment of Teflon tubing of constant cross-section. The integrated optical sensor informs the control units of the presence of droplets to avoid jamming them by the closing gate. In contrast to existing pinch valves or valves with flexible diaphragms (Quake valves) or plungers, the valve that we here describe does not create any spikes of pressure or rapid displacements of liquid when it changes its state. As compared to existing microvalves based on rotary drums,[31–33] our valve combines full tightness and homogeneity of the material exposed to the liquids flowing through.

The architecture that we propose is optimized for robustness against imperfections in micromachining: all the critical dimensions and working surfaces of tightly cooperating parts are native surfaces of commercially available prefabricates and are not affected by custom microfabrication.

The valve may be used for on-demand separation of blocks of a microfluidic system. We have demonstrated effective isolation of sensitive operations on droplets from the variations in pressure or flow rate in other parts of a large fluidic system. Due to the complete separation of blocks isolated by the valves, it is even possible to clean and sterilize a certain section of the chip with harsh chemicals, while droplets with fragile microorganisms are incubated and processed in another section. We proved the tightness of the valve and demonstrated its usability in a complex, long-lasting experiment involving the evolution of hundreds of independent populations of microorganisms on a chip – no leakage nor cross-contamination of droplets were observed over weeks of continuous operation.

Our valve utilizes segments of standardized tubing made of FEP or PFA Teflon. The internal diameter of the channels may be easily changed, depending on the tubing – the only revision of the design is changing the diameter of a single hole drilled in the rotary disk. For the same OD, commercially available FEP tubes include ID of 0.1, 0.25, 0.3, 0.5, 0.6, 0.75 and 0.8 mm; a similar selection is available for PTFE and PFA. The idea of utilizing standardized Teflon tubing for circulating bioreactors in droplets is not new; however, the described systems[53–55] do not provide operations of splitting, merging and replenishing of droplets. These experiments could benefit from the gate valves, as well as from the modular junctions and sensors for use with standard tubing.

We hope that the described valve may also be inspiring for a broad community of chemists interested in automated tools for working with extremely aggressive chemicals, both in the segmented and single phase flow. The same technology, based on externally tightened rotary gates, may be used

for building multichannel valves[32] or column switching valves based on the construction of Rheodyne® sample injectors for HPLC. Although we described only an architecture with a single channel, the number and configuration of working channels in the valve may be easily changed. We successfully used the same technology for two channels that opened and closed simultaneously and for a two-channel three-state valve (Ch1 open and Ch2 closed, both closed, Ch1 closed and Ch2 open). Modification of the number of channels is straightforward; however, simultaneous closing of two asynchronous flows of droplets may be impractical due to the necessity of waiting until both gates are simultaneously clear of droplets.

The idea of introducing more complex fluidic structures into the valve itself may have broader implications. Even the simple valve that we described here already offers three flat layers, kept in tight contact, cut from one of the best materials in microfluidics – FEP Teflon. Adding new layers or extra surfaces is straightforward. Due to the clamping provided by external covers, the bonding is not necessary (however, the extra layers, outside of the outline of the rotary disk, may be additionally bonded – in this case, they could extend out of the margins of the valve covers). An example of a microfluidic chip composed of two machined surfaces of fluorosilanized glass, slidable with respect to each other with a thin layer of fluorinated oil in between, has been proposed 7 years ago by the research group of Ismagilov.[56] The idea has also been demonstrated in acrylic plastic[57] and shown to be capable of performing operation on droplets without any external source of pressure – solely by capillary action, initiated by sliding the plates to a target position.[58] It is potentially an interesting direction for further research to combine the ideas of the slipchip, traditional multilayer microfluidics, and droplet compatible valve into a common, whole Teflon system – for robust realizations of complex liquid handling protocols for applications in biotechnology or chemistry. In fact, instead of integrating valves into microfluidic systems, one could think of integrating microfluidic systems onto the sliding surfaces of valves, similar to the one presented here or larger, more complex ones. The approach might provide for miniaturization, as it would allow the limitation of the mechanical infrastructure to the valve itself, eliminating all the typically indispensable automated sources of flow or pressure.

4 Materials and methods

4.1 Parts of the valve

The internal covers and central layer including the rotary disk with a gate (Fig. 2) were cut from 2.3 mm thick sheets of Symalit® FEP (Quadrant Group). The mechanical data of this material are as follows: hardness ~55 durometer Shore D, Young modulus ~350 MPa. The fluidic channels and ports were made of FEP tubes, ID = 0.8 mm, OD = 1.6 mm, BOLA® (brand of Bohlender GmbH), product number S 1815-04. For the external covers, we used two different materials: transparent covers were cut from a 10 mm thick polycarbonate sheet, Makrolon®, and the non-transparent ones (with optical sensors) from an extruded 9.5 mm PMMA sheet, Acrylite® (Evonik Industries), opaque black. Optic fibers (hard clad silica multimode optical fiber, 200 μm core, 400 μm total diameter (with buffer), Thorlabs®, product number FG200UCC) were glued by epoxy laminating resin MGS L285 (Hexion) into a stainless steel 21 gauge needle (OD 0.82 mm and ID 0.51 mm). After hardening of the resin, the needle with the fiber was cut and polished by a fine diamond grinding wheel and tightly placed into the metering hole in the external cover of the valve so that its tip touches the wall of the tubing. The sealing elements visible in Fig. 2 included X-rings (also called quad-rings) for sealing the shaft (2.57 × 1.78 mm, Viton 51414) and O-rings (24 × 1 mm, NBR 70 (between the FEP spacer in the central layer and internal covers), 24 × 1.5 mm, NBR70 (between the internal and external covers), and 1.5 × 1 mm, NBR 70 (O-rings used as springs to press internal covers towards the movable disk)). The dimensions of the grooves for large O-rings must be according to the manufacturer's specification; in particular, for 24 × 1 mm NBR-70 O-rings, the depth of the groove should be 0.75 mm. However, the groove depth for the smallest O-ring (1.5 × 1 mm) should be larger – from 0.8 to 0.9 mm, depending on the actual size and hardness of the O-ring. This depth is crucial for the balance between the requirement of internal tightness of the valve and avoiding excessive friction. Some of fluorinated oils may cause swelling and extraction of plasticizers from elastomers used for production of O-rings, esp. those that are sold as "oil-resistant", *e.g.* made from Viton®. Therefore, we recommend testing the compatibility of the materials by placing the tested O-ring in hot oil for several days and comparing its weight and size after and before the test. Immediately after removing from the oil bath, the tested element should be wiped with a dry paper towel; dark residues mean that the materials are not compatible. The rotary shaft was made of a round stainless steel rod of 3 mm diameter, drilled perpendicularly for the tight placement of a 0.8 mm pin (hardened steel). Precision ball bearings 683 EZO, 3 mm ID, 6 mm OD, 2 mm height, were used due to their lower demand on machining precision as compared to plain bearings. As a rotary actuator/drive, we used an RC servomotor HS-65MG (HiTec) with a torque of up to 0.22 N m, a speed of rotation of up to 9.5 rad s^{-1}, and dimensions of 11.5 × 30 × 26 mm (recommended for "heavy duty" applications, in contrast to many smaller models). Servo horns, levers, and sticks (to transmit torque from the rotary actuator to the shaft of the valve) should be adapted to the type of servo; these parts are widely available in RC-model shops. Prior versions of the rotary valve, based on Fig. 1A, were made of round PFA and FEP rods of diameters 3.175, 6.35 and 9.53 mm, Afton Plastics, and 4.8 mm thick FEP sheets distributed by Professional Plastics. The profiles of the cut of the tubing and the neighboring FEP cover were measured using a Bruker Countour GT-K0 optical profilometer (installed objectives 5× and 50×), and the data were processed using Gwyddion free software. Cutting and milling of all materials were carried out using a

general use 3-axis CNC milling machine (ErgWind MFG-4025P) with flat bottomed single flute end-mill cutters, optimized for Teflon and printed circuit boards (Performance Micro Tools, ET-1-0312-S). The holes for fiber ports were drilled using HSS drill bits of extended reach, long enough to drill holes for optical fibers from one side (to enhance the collinearity of both fibers). An Excel #17 chisel edge blade (single bevel with a bevel angle of 14° and a blade angle of 90°) was used for cutting the tubes in plane with internal covers – as in Fig. 2D.

4.2 Parts of the micro-droplet chemostat system

All valves and sensors were controlled by using a custom made electronic device based on two AT91SAM7S256 ARM 32-bit microcontrollers (Atmel). Materials for the operating block (see Fig. 4C) and wings of the micro-droplet chemostat system include FEP tubing, as in sec. 4.1, custom made modular T-junctions and cross-junctions (see the details in the ESI†) enabling snap-on connections of FEP tubing without a step change in ID, 2.3 mm thick sheets of Symalit® FEP (Quadrant Group), and custom made fiber optic sensors (boxes of white PTFE Teflon in Fig. 4C).

As for the inlet valves, we use custom modified[50] electromagnetic valves (Sirai V165 v16), with bistable solenoids (Z070D), driven by custom made electronics. These valves are equipped (in a downstream side) with up to 2 meters long stainless steel capillaries of ID = 0.2 mm, to increase their hydraulic resistance highly above a typical resistance of the driven system. As a result, the flow rate in the open valve depends almost solely on the inlet pressure and not on the other flow rates in different parts of the system.

The outlet valves are of the same type as inlet valves, yet without capillaries. As opposed to inlet valves, the resistance of ports and connections of an outlet valve must be as small as possible, to minimize the fluctuation of the flow rate caused by randomly chopped droplets in the outgoing ducts.

As the continuous liquid, we used fluorinated oil (HFE-7500) with 0.01% (w/w) of custom made surfactant (PFPE–PEG–PFPE, synthesized in Chemipan, Poland). Luria-Bertani (LB) was used as the medium, and wild-type *Escherichia coli*, strain K-12, served as model bacteria.

Acknowledgements

This project was financed within European Research Council Starting Grant 279647. Slawomir Jakiela acknowledges financial support from the National Science Center under grant Opus 8 no. 2014/15/B/ST4/04955.

References

1 M. G. Simon and A. P. Lee, in *Microdroplet Technology*, ed. P. Day, A. Manz and Y. Zhang, Springer, New York, 2012, ch. 2, pp. 23–50.
2 P. M. Korczyk, L. Derzsi, S. Jakiela and P. Garstecki, *Lab Chip*, 2013, **13**, 4096–4102.
3 T. S. Kaminski, K. Churski and P. Garstecki, in *Microdroplet Technology*, ed. P. Day, A. Manz and Y. Zhang, Springer, New York, 2012, ch. 5, pp. 117–136.
4 K. W. Oh and C. H. Ahn, *J. Micromech. Microeng.*, 2006, **16**, R13–R39.
5 A. K. Au, H. Lai, B. R. Utela and A. Folch, *Micromachines*, 2011, **2**, 179.
6 K. W. Oh, R. Rong and C. H. Ahn, *J. Micromech. Microeng.*, 2005, **15**, 2449.
7 C. R. Tamanaha, L. J. Whitman and R. J. Colton, *J. Micromech. Microeng.*, 2002, **12**, N7.
8 M. A. Unger, H.-P. Chou, T. Thorsen, A. Scherer and S. R. Quake, *Science*, 2000, **288**, 113–116.
9 H. Willaime, V. Barbier, L. Kloul, S. Maine and P. Tabeling, *Phys. Rev. Lett.*, 2006, **96**, 054501.
10 J.-H. Choi, S.-K. Lee, J.-M. Lim, S.-M. Yang and G.-R. Yi, *Lab Chip*, 2010, **10**, 456–461.
11 T. Thorsen, S. J. Maerkl and S. R. Quake, *Science*, 2002, **298**, 580–584.
12 S. H. Jin, H.-H. Jeong, B. Lee, S. S. Lee and C.-S. Lee, *Lab Chip*, 2015, **15**, 3677–3686.
13 D. H. Yoon, D. Wakui, A. Nakahara, T. Sekiguchi and S. Shoji, *RSC Adv.*, 2015, **5**, 2070–2074.
14 A. Jamshaid, M. Igaki, D. H. Yoon, T. Sekiguchi and S. Shoji, *Micromachines*, 2013, **4**, 34.
15 D. H. Yoon, J. Ito, T. Sekiguchi and S. Shoji, *Micromachines*, 2013, **4**, 197.
16 A. Mata, A. J. Fleischman and S. Roy, *Biomed. Microdevices*, 2005, **7**, 281–293.
17 K. J. Regehr, M. Domenech, J. T. Koepsel, K. C. Carver, S. J. Ellison-Zelski, W. L. Murphy, L. A. Schuler, E. T. Alarid and D. J. Beebe, *Lab Chip*, 2009, **9**, 2132–2139.
18 J. N. Lee, C. Park and G. M. Whitesides, *Anal. Chem.*, 2003, **75**, 6544–6554.
19 M. W. Toepke and D. J. Beebe, *Lab Chip*, 2006, **6**, 1484–1486.
20 P. Shivapooja, Q. Wang, L. M. Szott, B. Orihuela, D. Rittschof, X. Zhao and G. P. Lopez, *Biofouling*, 2015, **31**, 265–274.
21 E. Berthier, E. W. K. Young and D. Beebe, *Lab Chip*, 2012, **12**, 1224–1237.
22 M. D. Borysiak, K. S. Bielawski, N. J. Sniadecki, C. F. Jenkel, B. D. Vogt and J. D. Posner, *Lab Chip*, 2013, **13**, 2773–2784.
23 C. F. Carlborg, T. Haraldsson, K. Oberg, M. Malkoch and W. van der Wijngaart, *Lab Chip*, 2011, **11**, 3136–3147.
24 F. Ilievski, A. D. Mazzeo, R. F. Shepherd, X. Chen and G. M. Whitesides, *Angew. Chem., Int. Ed.*, 2011, **50**, 1890–1895.
25 R. F. Shepherd, F. Ilievski, W. Choi, S. A. Morin, A. A. Stokes, A. D. Mazzeo, X. Chen, M. Wang and G. M. Whitesides, *Proc. Natl. Acad. Sci. U. S. A.*, 2011, **108**, 20400–20403.
26 A. A. Nawaz, X. Mao, Z. S. Stratton and T. J. Huang, *Lab Chip*, 2013, **13**, 1457–1463.
27 P. N. Nge, C. I. Rogers and A. T. Woolley, *Chem. Rev.*, 2013, **113**, 2550–2583.
28 W. Zhang, S. Lin, C. Wang, J. Hu, C. Li, Z. Zhuang, Y. Zhou, R. A. Mathies and C. J. Yang, *Lab Chip*, 2009, **9**, 3088–3094.
29 K. S. Lee and R. J. Ram, *Lab Chip*, 2009, **9**, 1618–1624.

30 Y. Temiz, R. D. Lovchik, G. V. Kaigala and E. Delamarche, *Microelectron. Eng.*, 2015, **132**, 156–175.
31 T. Hasegawa, K. Nakashima, F. Omatsu and K. Ikuta, *Sens. Actuators, A*, 2008, **143**, 390–398.
32 W. Wang, J. J. Lu, C. Gu, L. Zhou and S. Liu, *Anal. Chem.*, 2013, **85**, 6603–6607.
33 R. Luharuka and P. J. Hesketh, *J. Micromech. Microeng.*, 2008, **18**, 035015.
34 B. Ameduri, B. Boutevin and G. Kostov, *Prog. Polym. Sci.*, 2001, **26**, 105–187.
35 B. Ameduri and B. Boutevin, *J. Fluorine Chem.*, 2005, **126**, 221–229.
36 A. Waldbaur, H. Rapp, K. Lange and B. E. Rapp, *Anal. Methods*, 2011, **3**, 2681–2716.
37 R. M. van Dam, *Ph.D. thesis*, California Institute of Technology, 2006.
38 S. Begolo, G. Colas, J.-L. Viovy and L. Malaquin, *Lab Chip*, 2011, **11**, 508–512.
39 S. Ebnesajjad and P. Khaladkar, *Fluoropolymer Applications in the Chemical Processing Industries: The Definitive User's Guide and Databook*, Elsevier Science, 2004.
40 S. Ebnesajjad, *Fluoroplastics, Volume 2: Melt Processible Fluoroplastics: The Definitive User's Guide*, Elsevier Science, 2002.
41 K. Ren, W. Dai, J. Zhou, J. Su and H. Wu, *Proc. Natl. Acad. Sci. U. S. A.*, 2011, **108**, 8162–8166.
42 T. W. de Haas, H. Fadaei and D. Sinton, *Lab Chip*, 2012, **12**, 4236–4239.
43 H. Zheng, W. Wang, X. Li, Z. Wang, L. Hood, C. Lausted and Z. Hu, *Lab Chip*, 2013, **13**, 3347–3350.
44 J. G. Bomer, A. V. Prokofyev, A. van den Berg and S. Le Gac, *Lab Chip*, 2014, **14**, 4461–4464.
45 W. H. Grover, M. G. von Muhlen and S. R. Manalis, *Lab Chip*, 2008, **8**, 913–918.
46 P. A. Willis, B. D. Hunt, V. E. White, M. C. Lee, M. Ikeda, S. Bae, M. J. Pelletier and F. J. Grunthaner, *Lab Chip*, 2007, **7**, 1469–1474.
47 K. C. Bhargava, B. Thompson and N. Malmstadt, *Proc. Natl. Acad. Sci. U. S. A.*, 2014, **111**, 15013–15018.
48 S. Jakiela, T. S. Kaminski, O. Cybulski, D. B. Weibel and P. Garstecki, *Angew. Chem., Int. Ed.*, 2013, **52**, 8908–8911.
49 E. Verneuil, M. Cordero, F. Gallaire and C. N. Baroud, *Langmuir*, 2009, **25**, 5127–5134.
50 K. Churski, P. Korczyk and P. Garstecki, *Lab Chip*, 2010, **10**, 816–818.
51 K. Churski, M. Nowacki, P. M. Korczyk and P. Garstecki, *Lab Chip*, 2013, **13**, 3689–3697.
52 S. P. Barrett, *Epidemiol. Infect.*, 1988, **100**, 91–100.
53 K. Martin, T. Henkel, V. Baier, A. Grodrian, T. Schon, M. Roth, J. Michael Kohler and J. Metze, *Lab Chip*, 2003, **3**, 202–207.
54 L. Jiang, L. Boitard, P. Broyer, A.-C. Chareire, P. Bourne-Branchu, P. Mahé, M. Tournoud, C. Franceschi, G. Zambardi, J. Baudry and J. Bibette, *Eur. J. Clin. Microbiol. Infect. Dis.*, 2016, **35**, 415–422.
55 S. P. Damodaran, S. Eberhard, L. Boitard, J. G. Rodriguez, Y. Wang, N. Bremond, J. Baudry, J. Bibette and F.-A. Wollman, *PLoS One*, 2015, **10**, e0118987.
56 W. Du, L. Li, K. P. Nichols and R. F. Ismagilov, *Lab Chip*, 2009, **9**, 2286–2292.
57 Y. Zhao, F. Pereira, A. J. deMello, H. Morgan and X. Niu, *Lab Chip*, 2014, **14**, 555–561.
58 R. R. Pompano, C. E. Platt, M. A. Karymov and R. F. Ismagilov, *Langmuir*, 2012, **28**, 1931–1941.

